Fast Eight-Domain Patterned Vertical Alignment Mode with Reactive Mesogen for a Single-Transistor-Driving

You-Jin Lee[1], Soo In Jo[2], Jae-Hoon Kim[1,2], and Chang-Jae Yu[1,2*]

[1] *Department of Information Display Engineering, Hanyang University, Seoul 133-791, Korea*
[2] *Department of Electronics and Communications Engineering, Hanyang University, Seoul 133-791, Korea*

Received November 24, 2009; accepted January 27, 2010; published online March 5, 2010

We proposed a wide-viewing patterned vertical alignment (PVA) mode with eight-domains driven by a single transistor. The eight-domain PVA mode was fabricated by introducing two different pretilt angles in a pixel using polymerized reactive mesogens (RMs) within alignment layer. The pretilt angles are simply controlled by an applied voltage during illumination of ultraviolet light for polymerization of the RMs. In addition, the polymerized RMs give rise to defect-free transition in our advanced PVA mode and thus fast response can be achieved over whole grey level.

DOI: 10.1143/JJAP.49.030209

The expansion of the digital television (TV) market demands a large-size flat panel display (FPD) TV with high display performance. Compared to other FPD-TVs, thin film transistor liquid crystal displays (TFT-LCDs) have the advantages of high resolution, light weight, slim size, and low power consumption. However, the drawbacks of TFT-LCDs are slow response time, limited viewing angle performance, and high manufacturing cost. Various LC modes have been developed for high display performance,[1–6)] and among them, a patterned vertical alignment (PVA) mode is at the leading position due to their high contrast ratio at the on-axis direction with chevron type electrode for generating the multi-domains.[5,6)] However, four-domain structure has limitation to get the high image quality in off-axis directions without optical compensation film. Recently, a super-PVA mode with an additional TFT for each pixel was proposed.[7,8)] The super-PVA mode divides each pixel into two parts with each TFT and thus it has twice as many domains as a conventional PVA mode. However, complicated driving scheme, low aperture ratio due to additional TFTs, and cost increase are inevitably involved in the super-PVA mode.

In our previous work, we proposed the surface controlled PVA (SC-PVA) mode using ultraviolet (UV) curable reactive mesogen (RM) mixed with vertical alignment material.[9)] In the SC-PVA mode, the RM monomers in the alignment layer are polymerized along the LC directors by UV exposure under an applied voltage. The directional polymerization of the RMs produced the rotational preference in an azimuthal direction during switching the LC molecules. In this configuration, the response time could be considerably reduced due to defect-free transition in the VA mode.

In this paper, we proposed the advanced SC-PVA mode which has improved viewing angle characteristics on off-axis directions with eight-domains similar to the super-PVA mode. The eight-domain SC-PVA mode was prepared with introducing two different pretilt angles in a single pixel driven by a single transistor. The different pretilt angles were produced in a pixel by polymerized RMs which were cured with different applying voltage during UV illumination. In addition, the predetermination of the LC switching directions by the polymerized RMs gave rise to the fast response time over whole grey levels.

*E-mail address: cjyu@hanyang.ac.kr

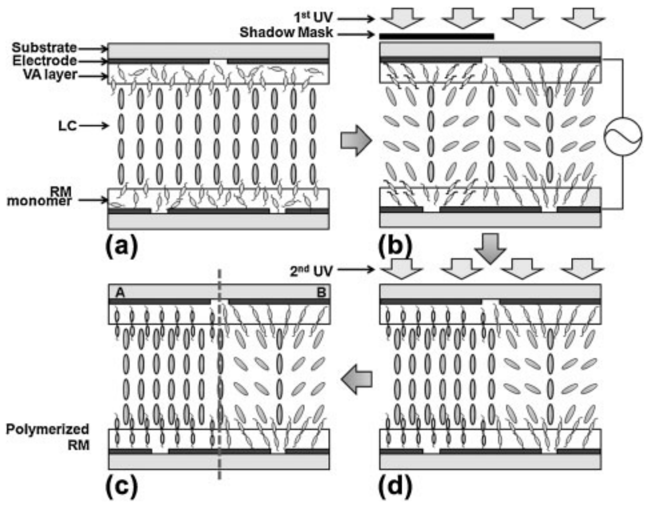

Fig. 1. The schematic diagram of our advanced SC-PVA mode and the fabrication processes.

Figure 1 shows a schematic diagram of fabrication process for the advanced SC-PVA mode with the different pretilt angles in a single pixel. The RM monomer (BASF) and photoinitiator (Ciba Chemical IRGACURE 651) was mixed in vertical alignment material (JSR AL60101). The mixed alignment layer was coated on the ITO substrate with chevron type electrode pattern for generating oblique electric field and prebaked at 80 °C for 10 min followed by curing at 180 °C for 1 h. The cell thickness of the assembled substrates was maintained by the use of 3 μm glass spacers. The LC (Merck MLC-6610, $\Delta\epsilon = -3.1$ and $\Delta n = 0.0996$) were injected into the assembled cell by capillary action in the isotropic phase. At an initial state, the LC molecules were aligned vertically and the RM mononers were distributed randomly in the alignment layer as shown in Fig. 1(a). When a voltage was applied larger than a certain threshold voltage, the LC molecules fell down perpendicular to the electric field, similarly to a conventional PVA mode, and the RM monomers were aligned along the LC molecules. At this situation, the area B of LC cell was irradiated as the first step UV exposure through a photo mask and thus the RM monomers were polymerized in the alignment layer at exposed area B [Fig. 1(b)]. The polymerized RMs produce the pretilt angle whose azimuthal direction are determined by the direction of the fringe field

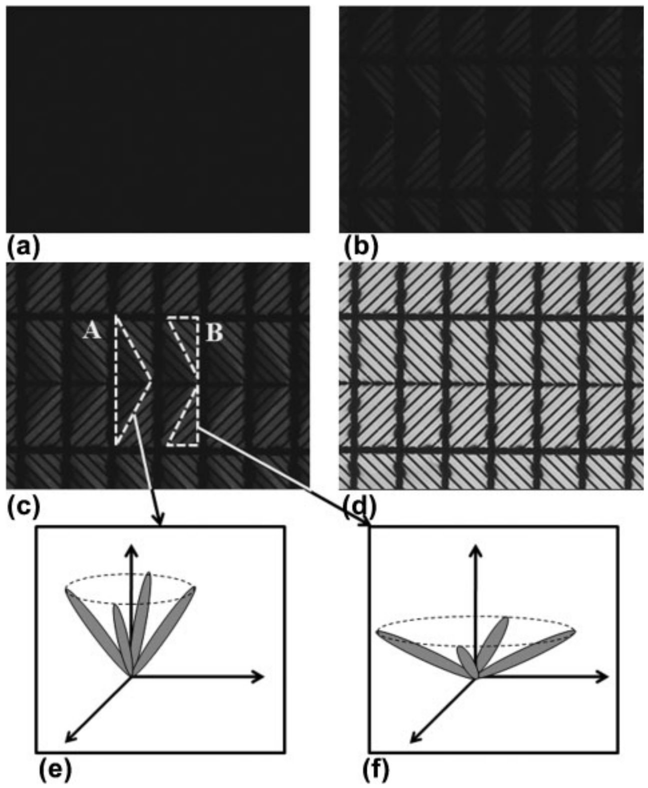

Fig. 2. Microscopic textures under crossed polarizers with (a) 0, (b) 3.2, (c) 4.5, and (d) 10 V, respectively. Schematic diagrams of LC directors with an applied voltage for area (e) A and (f) B, respectively.

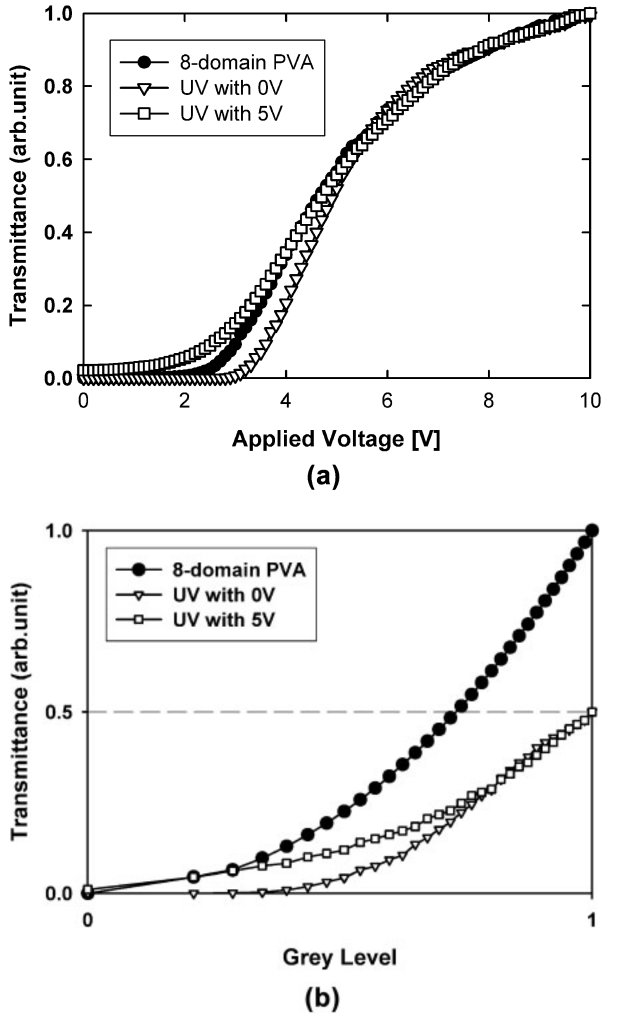

Fig. 3. (a) The voltage–transmittance characteristics and (b) the grey–transmittance characteristics with gamma-correction of $\gamma = 2.2$.

by UV exposure in the presence of the applied voltage.[9] To produce a different pretilt angle, the second step UV light was exposed to the whole cell area [Fig. 1(d)] applying a different voltage. In the area B, the RMs were already polymerized and there was no change. In the area A, however, the remained RM monomers produce the different pretilt angle from the area B during UV curing process due to a different applied voltage. In our experience, the 5 and 0 V were applied during the first and second step UV exposure processes, respectively. It should be noted that the pretilt angles depend on the curing voltage, exposure time, RM concentration, and so on. The pretilt angles are fixed at whole region after curing the RM monomers completely and removing the curing voltage as shown in Fig. 1(c). Finally, the two kind of pretilt angles are produced in a pixel, which can make the eight-domain in the PVA mode to improve the viewing angle characteristics. For large electro-optical difference between two regions, high pretilt angles could be introduced in one region with high applied voltage during curing RM monomers and high concentration ratio of RM polymers in the alignment layer, but that make possible the light leakage in the dark state resulting in a lower contrast ratio. Therefore, the optimized conditions were required for reach high display performance.

Figure 2 shows the microscopic textures under crossed polarizers after two-step UV exposure with triangular shape photo mask. In the absence of the applied voltage, the LC molecules aligned vertically in both areas and thus they are indistinguishable to each other due to the slight difference of pretilt angles [Fig. 2(a)]. Figures 2(b), 2(c), and 2(d) are shown the textures for 3.2, 4.5, and 10 V, respectively. As increasing the applied voltage, the LC molecules are fallen down to the substrate. However, the falling degrees at each area A and B are different due to their different pretilt angles, so we got different transmittance with the same applied voltage. Figures 2(e) and 2(f) show the schematic diagram of the LC directions. Since each area has the four-domains like the conventional PVA cell, we obtained eight-domains with different azimuthal and polar direction, which make possible to improve the viewing angle characteristics in off-axis directions.

Figure 3(a) shows the voltage–transmittance (V–T) characteristics for the area A, B, and total area of the eight-domain PVA cell. Due to low pretilt angle against the substrate, the threshold voltage of the area B is lower than one of the area A and the V–T curves are shifted to left. Therefore, the eight-domain PVA mode which has two regions of high and low pretilt angles, the curve exists in the middle of two V–T curves. In our cell condition, the contrast ratio for our eight-domain PVA cell was measured to be 261 : 1, which slightly decreased in comparison to the conventional PVA cell (296 : 1, in the same cell conditions as the eight-domain PVA cell). Figure 3(b) represents gamma characteristics ($\gamma = 2.2$) when the cell is viewed from on-axis. Since two areas of A and B shows different luminance characteristics for grey levels due to different

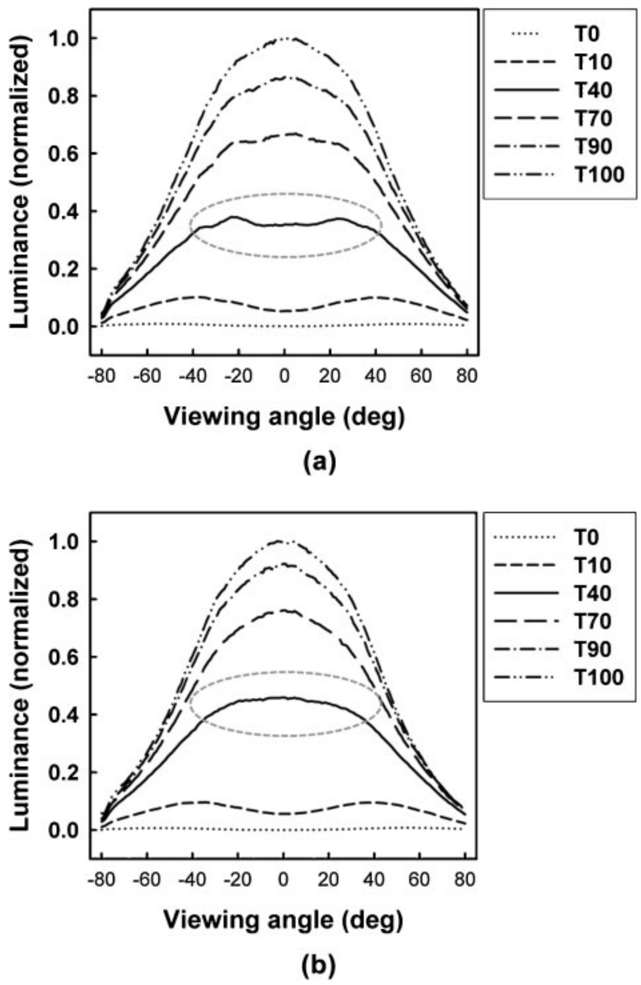

Fig. 4. Comparison of brightness viewing characteristics between (a) a conventional four-domain PVA mode and (b) the advanced eight-domain PVA mode for 45° with respect to polarizers.

tilting angles, the viewing angle characteristics can be compensated each other from off-axis. In Fig. 4, we compared the brightness viewing angle characteristics between a conventional four-domain PVA cell and the advanced eight-domain PVA cell. The measured azimuthal direction was 45° with respect to polarizers. For the conventional PVA cell [Fig. 4(a)], the grey inversions are appeared at the middle grey level. On the contrary, our eight-domain cells are overcome this problem, as shown in Fig. 4(b). However, in low grey levels, the effect is very small because the difference of tilting angle is not so large. If we increase the applied voltage during UV curing (i.e., increase the pretilt angle) in area B, the difference of tilting angle could be increased but the contrast ratio could be decreased due to a light leakage by the introduction of the effective retardation at dark state.

In the conventional super-PVA modes, the response time is still insufficient because of the reorientation processes of LC directors in the center of two overlapping electrodes (pixel and common electrodes). The director reorientation is originated from no fringe field and no preference of LC falling direction in the center of two overlapping electrodes. On the contrary, our advanced SC-PVA mode shows very fast response characteristics because the memorization of the azimuthal falling-down direction by polymerized RMs

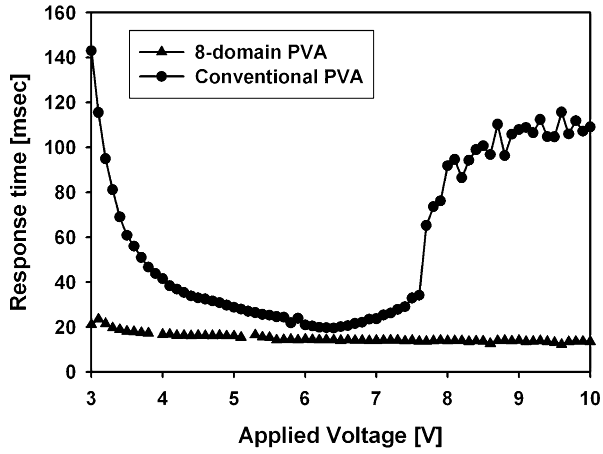

Fig. 5. Response time characteristics of the conventional PVA mode and our advanced PVA mode.

guides to the stable alignment state of the LC molecules without reorientation process, as similar to the SC-PVA mode.[9)] Figure 5 shows the response time characteristics as a function of applied voltage for our advanced SC-PVA mode cell and a conventional super-PVA mode cell, they have same cell parameters (i.e., same LC materials, electrode structures and cell gaps). In the advanced SC-PVA case, the response time is 17 ms at applied 7 V and is not much than 20 ms at whole grey levels, which is enough for moving pictures. If you use the overdriving technologies as commercial LC-TVs does,[10,11)] we could get faster response time.

In summary, we proposed the advanced eight-domain PVA mode by dynamic controlling the pretilt angles with the RMs for a single-transistor-driving. The polymerized RMs produced the pretilt angles governed by the applied voltage during UV illumination for polymerizing the RMs. The eight-domain structure was fabricated by alternating UV exposure applying the different voltages in a single pixel. In addition, the memorization of the falling direction by the polymerized RMs caused the fast response time. In this advanced SC-PVA cell, wide-viewing and fast response characteristics were realized without any additional TFT and/or capacitor in whole grey levels.

1) S. Yamauchi, M. Aizawa, J. F. Clerc, T. Uchida, and J. Duchen: SID Int. Symp. Dig. Tech. Pap. **20** (1989) 378.
2) S. Ohmuro, S. Kataoka, T. Sasaki, and Y. Koike: SID Int. Symp. Dig. Tech. Pap. **28** (1997) 845.
3) M. Oh-e and K. Kondo: Appl. Phys. Lett. **67** (1995) 3895.
4) S. H. Lee, S. L. Lee, and H. Y. Kim: Appl. Phys. Lett. **73** (1998) 2881.
5) K. Sueoka, H. Nakamura, and Y. Taira: SID Int. Symp. Dig. Tech. Pap. **28** (1997) 203.
6) K. H. Kim, K. Lee, S. B. Park, J. K. Song, S. N. Kim, and J. H. Souk: Proc. Int. Display Research Conf., Asia Display, 1998, p. 383.
7) S. S. Kim: SID Int. Symp. Dig. Tech. Pap. **35** (2004) 760.
8) S. S. Kim: SID Int. Symp. Dig. Tech. Pap. **36** (2005) 1842.
9) Y.-J. Lee, Y.-K. Kim, S. In Jo, J. S. Gwag, C.-J. Yu, and J.-H. Kim: Opt. Express **17** (2009) 10298.
10) B.-W. Lee, C. Park, S. Kim, M. Jeon, J. Heo, D. Sagong, J. Kim, and J. Souk: SID Int. Symp. Dig. Tech. Pap. **32** (2001) 1260.
11) J. K. Ong, K. E. Le, H. S. Chagn, S. M. Hong, M. B. Jun, B. Park, S. S. Seomun, K. H. Kim, and S. S. Kim: SID Int. Symp. Dig. Tech. Pap. **35** (2004) 1344.